Timing and localization of reconnection signatures – Is there a substorm model problem?

Dietmar Krauss-Varban and Homa Karimabadi

Department of Electrical and Computer Engineering, University of California, San Diego, La Jolla, California, USA

Received 1 October 2002; revised 19 December 2002; accepted 12 February 2003; published 25 March 2003.

[1] Observations place ionospheric substorm onset signatures on field lines that map to the near-Earth plasma sheet, and field-aligned currents (FACs) are observed before dipolarization, equatorward of open field lines. The near-Earth neutral line (NENL) model, however, appears to suggest perturbations to originate from the *x*-line on newly reconnected field lines, which map to much higher latitudes. Its order of dipolarization, FACs, and subsequent ionospheric signatures contradicts the observations. Using large-scale kinetic simulations, we demonstrate that these "flaws" of the NENL model are misconceptions and that the timing and location of signatures in the model are indeed consistent with observations. In a thinned current sheet, energetic ions are virtually unmagnetized, get further energized when passing through the neutral sheet, and travel earthward quickly and close to the neutral sheet, thus providing a pathway for early substorm signatures at relatively low latitudes. *INDEX TERMS:* 2788 Magnetospheric Physics: Storms and substorms; 2744 Magnetospheric Physics: Magnetotail; 2716 Magnetospheric Physics: Energetic particles, precipitating; 2736 Magnetospheric Physics: Magnetosphere/ionosphere interactions; 2748 Magnetospheric Physics: Magnetotail boundary layers.

Citation: Krauss-Varban, D., and H. Karimabadi, Timing and localization of reconnection signatures – Is there a substorm model problem?, *Geophys. Res. Lett.*, *30*(6), 1308, doi:10.1029/2002GL016369, 2003.

1. Introduction

[2] Magnetospheric substorms [*Akasofu*, 1964; *Baker et al.*, 1996] release energy stored in accumulated magnetic flux that originates from the dayside. Substorm onset was originally characterized as the sudden brightening of a discrete arc near the equatorward edge of the auroral zone [*Akasofu*, 1964]. Yet, no consensus exists on how this energy release is triggered. Details of the processes leading to field-aligned currents (FACs) and the timing and localization of signatures at geostationary orbit and in the ionosphere are poorly understood. In the near-Earth neutral line (NENL) model [*Hones*, 1976; *Hones et al.*, 1984; *Baker et al.*, 1996], the energy release is both initiated and accomplished through magnetic reconnection of the field lines in the mid-tail. In alternate models, other processes closer to Earth lead to current disruption (CD) and trigger the substorm [e.g., *Lui*, 1996].

[3] Mapping of ionospheric onset signatures along the field lines into the equatorial tail place their origin with the current wedge, between 6 and 12 R_E. *Samson et al.* [1992] and other ground-based studies have used line emissions from the background proton aurora to map the inner plasmasheet to the auroral ionosphere. Such studies appear to show that the onset process maps to the near-tail equatorial region – the transition from dipolar to stretched field lines. In the ionosphere, this is 4°–6° equatorward of the region of open field lines. Emissions related to energetic electrons subsequently move poleward over a period of a few minutes. This is interpreted as a progression of signatures from farther down the tail [*Friedrich et al.*, 2001], indicating that lobe reconnection sets in 1 to 5 minutes later.

[4] Additional support for the CD model appears to come from early formation of FACs equatorward of the open field line region [*Lopez et al.*, 1991; *Friedrich et al.*, 2001], and delayed arrival of dipolarization [*Lopez et al.*, 1990; *Ohtani et al.*, 1999; *Friedrich et al.*, 2001].

[5] The modern NENL model attempts to explain the above near-Earth placement via the pile-up of earthward transported plasma and flux close to the inner edge of the plasmasheet [*Haerendel*, 1992; *Shiokawa et al.*, 1998], where FACs are generated during the plasma deceleration process. Still, in the light of the above observations, the NENL model appears to have several serious flaws: Firstly, it requires that dipolarization has progressed all the way to the inner edge of the plasmasheet before significant signatures are generated near Earth. Secondly, important signatures generated during deceleration would presumably be on newly-reconnected or even on lobe field lines, which map to much higher latitudes than observed. Thirdly, the order of dipolarization, FACs, and subsequent ionospheric processes contradicts the above observations.

[6] However, a plain consequence of extreme and extended tail thinning is that magnetic footpoints of the pre-onset equatorial region of the near tail and those of the NENL are very close to each other [*Baker et al.*, 1996]. Thus, mapping efforts are notoriously difficult [e.g., *Wanliss et al.*, 2000]. Also, progressive arrival of signatures from farther downtail can be due to time-of-flight effects rather than signifying a tailward propagating perturbation.

[7] We have set out to investigate the relative timing and location of various substorm-related signatures in self-consistent kinetic simulations, which do not share the problems and inaccuracies of conventional mapping procedures. We pose the question whether under closer examination, the NENL model could in fact be in agreement with the above observations.

2. Simulation Model

[8] It is widely held that the relevant initial processes and signatures concerning the release of the stored magnetotail

0094-8276/03/2002GL016369$05.00

energy take place in about 3 to 5 minutes [*Machida et al.*, 1999; *Newell et al.*, 2001]. This timeframe, and the fact that ion kinetic processes dominate the post-onset physics in the magnetotail, make hybrid simulations (kinetic ions, electron fluid) particularly well suited.

[9] Our simulations are 90 × 36 × 120 cells large in the *GSM x*, *y*, and *z* directions, respectively, with a cell size of 1/4 proton inertial length c/ω_p in the *z*-direction, and $1c/\omega_p$ in *x* and *y*, with 30 particles per cell on average. All quantities are normalized to lobe values close to Earth (density: n_o, magnetic field: B_o); $6c/\omega_p$ is taken to be 1 R_E, and the inverse proton cyclotron frequency is Ω_p^{-1} = 0.75s. The time step is 0.025 Ω_p^{-1}, with a total run time of about 3min. real time. There are two ion species (*c*, *h*) and electrons (*e*): cold lobe plasma with $\beta_c = \beta_e = 0.01$ and hot plasmasheet protons with $T_{ho}/T_{co} = 50$ that carry part of the cross-tail current. The cold plasma background is non-uniform in the center: $n_c = n_o - n_h$ for $n_h/n_o < 0.9$, and $n_c/n_o = 0.1$ for larger n_h.

[10] We are not concerned with the reconnection onset mechanism and detailed physics of the diffusion region. Instead, we rely on the overwhelming observational evidence that places the NENL at around $x = -18$ R_E to -21 R_E [e.g., *Miyashita et al.*, 1999; *Ueno*, 1999], and set artificial resistivity at $x = -18$ R_E to achieve reconnection. The diffusion region has 1/*cosh* dependence with characteristic width of $4c/\omega_p$ in *y*. The boundary conditions are of freely floating inflow-outflow type [*Krauss-Varban et al.*, 1999] except at the earthward boundary, where the plasmasheet ions reflect to allow the plasma and flux to build up during dipolarization.

[11] It is generally accepted that before substorm onset, the plasmasheet stretches and thins to below the thermal proton gyro scale and over a wide range of distances [e.g., *Pulkkinen et al.*, 1999; *Wanliss et al.*, 2000]. Here we are interested in the early development before and up to the point when the dipolarization front reaches geostationary orbit. Unfortunately, there exist no realistic equilibrium that includes the transition from dipolar to stretched field lines. For these reasons, we concentrate on the region $x = -7$ R_E to -22 R_E, and use the *Birn-Zwingmann* equilibrium with a small modification to reduce B_z/B_o around the diffusion region and to lessen the flaring of the field lines: $F'(x) = F(x) + \varepsilon/cosh(x/\lambda)$. Here, $F(x) = (1 + b(x_{max} - x)/(\nu L))^{-\nu}$ is the equilibrium function defined in *Zwingmann et al.* [1990] with parameters $b = 0.025$ and $\nu = 0.6$; the current sheet thickness is $L = 2c/\omega_p$, x_{max} is the earthward boundary, $\lambda = 35c/\omega_p$, and $\varepsilon = 0.23$ (see next section for the resulting magnetic field profile).

3. Results

[12] Figure 1 shows the equatorial B_z vs. radial distance over time, 1/2 R_E west of the midnight meridian, where it is strongest due to 3-D effects. It progresses as a steepening front with two time scales, at 2.9 R_E/min. for the first minute, and almost twice as fast (5.1 R_E/min.) after the onset of lobe reconnection. The earthward boundary is reached at 157s. The simulation does not address subsequent tailward expansion of dipolarization associated with pile-up [see, e.g., *Hesse and Birn*, 1991]. Also, since outside the reconnection region there is no diffusion in the simulation, the plasma cannot pile up without also transporting flux earthward.

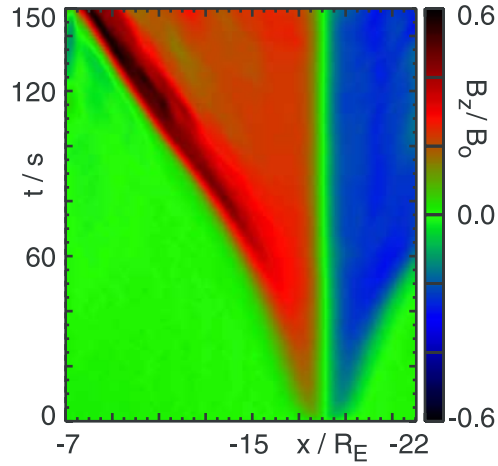

Figure 1. Normalized *z*-component of the equatorial magnetic field near midnight meridian vs. radial distance and time after reconnection onset.

[13] Ions are efficiently energized in the post-reconnection plasmasheet and quickly propagate earthward [*Arzner and Scholer*, 2001]. The acceleration takes place in single passes of the neutral sheet over a wide and increasing range of distances away from the diffusion region. As a consequence of this acceleration process, the energized ions are not limited to the plasmasheet boundary layer. A good quantity that summarizes energization and transport weighted with density is the heat flux. Figure 2 displays a cross section close to the midnight meridian of the hot (original plasmasheet) ion *x*-velocity v_{xh}, density n_h, and parallel heat flux q_h, normalized with n_o, the Alfvén velocity v_A, and T_{ho}, at two times. A few field lines (neglecting B_y) around the reconnection site are included for orientation. Hot ions start to flow around the denser part of the plasmasheet, eventually attaining Alfvén speed and forming a new boundary layer. However, as is evident, they are very dilute. At the same distance, the bulk of the plasmasheet is still largely unaffected. Hot ions forced closer into the current layer are not magnetized, get further energized when passing through the neutral sheet, and thus can quickly propagate earthward very close to the neutral sheet [cf. *Baker et al.*, 1996]. This is evident in the associated heat flux. On the other hand, the dilute boundary layer ions do not initially contribute to the heat flux; their innermost and densest part only later forming a segment of the heat flux that moves to larger equatorial distances over time.

[14] Due to the presence of fluctuations and a mild kink instability, the two hemispheres show some differences. For the remainder of this paper we will concentrate on the south, which is slightly less perturbed. To allow for a clean evaluation of the pertinent initial processes and to avoid the turbulence close to the earthward boundary, we concentrate on a distance of 10 R_E.

[15] Figure 3 shows profiles of the *z* and *x*-components of the magnetic field and the hot and cold ion parallel heat fluxes (q_h and q_c; negative is earthward) at this distance, versus *z* and time. The dipolarization front arrives between

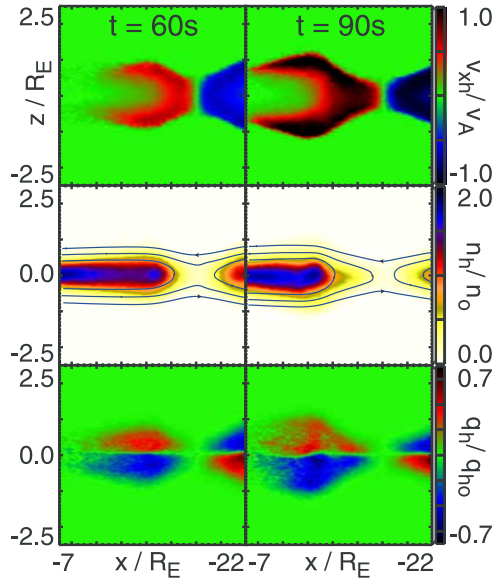

Figure 2. Near midnight-meridian cut of hot ion velocity v_{xh}, density n_h, and parallel heat flux q_h at two times, as indicated, with a few field lines around reconnection site.

110s and 120s, depending on equatorial distance, with only little perturbations of the main (x) magnetic field until then. The energized hot ions arrive about 40s before the energized lobe ions, which in turn arrive ~20s before the dipolarization front. Lobe ions are more efficiently energized, but their effective temperature remains an order of magnitude lower. Both energized species, in particular the hot ions, arrive first close to the equator (between 0.0 and 0.5 R_E; i.e., in the plasmasheet), and tend to appear at larger equatorial

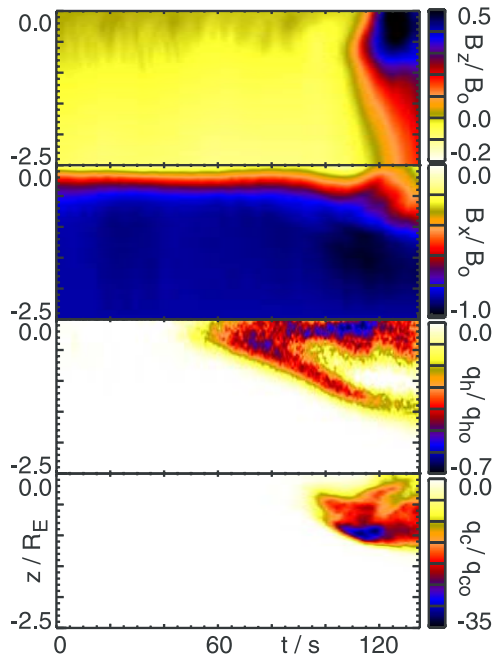

Figure 3. z-profile of B_z and B_x magnetic field components and energized plasmasheet (q_h) and lobe ion (q_c) heat fluxes near midnight meridian at 10 R_E distance, vs. time after reconnection onset (southern hemisphere).

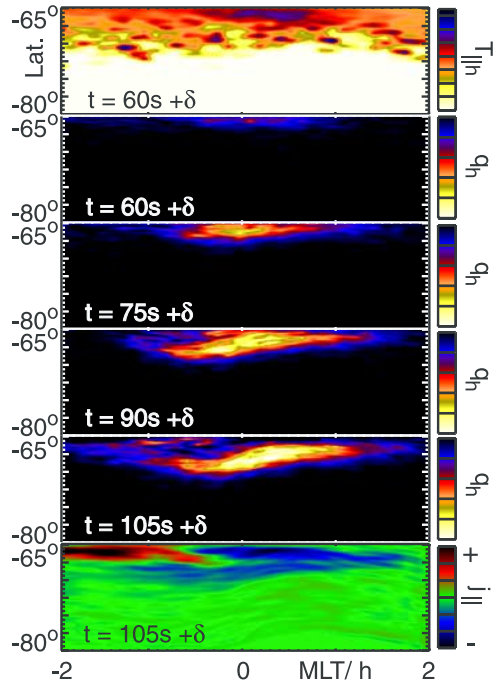

Figure 4. Near-Earth projection of parallel temperature, heat fluxes, and parallel current $j_\parallel$ (<0: earthward) at various times after reconnection onset, with time delay δ from 10 R_E to near-Earth location, vs. latitude (southern hemisphere) and local time from midnight.

distances at later time, in agreement with Figure 2. With only little perturbations of the magnetic field until ~120s, this signature is essentially undisturbed by changes in the field topology. With the normalization ratio T_{ho}/T_{co} = 50, both species' maximum heat fluxes are actually identical.

[16] Given the ionospheric observations of interest, it is instructive to look at the particle and FAC signatures mapped close to Earth. A simple stretched field model leads to a region about 4 hours of local time wide, and extending from −80° to −65° in latitude (southern hemisphere; equatorward boundary maps to current sheet center at −10 R_E). Earthward moving energetic ions may precipitate, cause enhanced ion aurora, generate secondary electrons, or may be involved in the generation of electron acceleration regions. Details of such processes are beyond the scope of this work. In Figure 4 we simply show the mapped location of the ions and parallel current $j_\parallel$, in arbitrary units. Times indicate an additional travel time to the ionosphere δ, which may be ~25s for the particles and ~50s for $j_\parallel$. The parallel temperature shows that the initial signature is at low (absolute) latitudes relative to a background, which may be interpreted as the background ion precipitation region. A more useful quantity is the heat flux, which confirms this location and shows penetration to higher latitudes over time, approximately reaching the poleward boundary of the background region ~45s later. Early in the simulation, the x-line maps approximately to this region (compare Figure 2). Between 90s and 105s, and still 15 to 30s before the arrival of the dipolarization front, a sizable parallel current develops in the tail (0.02 to 0.04MA over ~1 R_E^2; growing to ~twice as much at later times) that likewise maps to relatively low latitudes. A negative earthward and a positive

return current can be seen. Ionospheric signatures expected from these currents are consistent with common pre-midnight observations.

4. Summary

[17] Our work reveals that in a sufficiently stretched tail with a small B_z, plasmasheet and lobe ions that are energized after reconnection onset reach the near-Earth region quickly and initially close to the current sheet. Energetic ions arrive at geostationary orbit ~80s before the dipolarization front, and a sizable $j_{||}$ builds up about midway in time. When projected into the ionosphere, signatures start at relatively low latitudes, at the equatorward edge of background plasmasheet ion precipitation, moving to higher latitudes and to the poleward edge of this region in about 45s.

[18] Conventionally, such signatures are attributed to an onset mechanism that maps to near-Earth, with the later arrival at higher latitudes often ascribed to a tailward-traveling perturbation. We have demonstrated that these signatures are not in contradiction with the NENL model and that, in fact, this model properly accounts for a number of observations that previously were thought to be in agreement only with alternative onset models, placed at the inner edge of the plasmasheet.

[19] We emphasize that we have used a standard tail model with realistic parameters, such as an extended, thinned current layer and a small B_z in the vicinity of the diffusion region. We have executed a small number of parameter variations and see some dependence of the results on the current sheet thickness, strength of B_z, plasmasheet density, and extent of the diffusion region in y. More work is required to quantify such dependencies. Also, it is desirable to include a better equilibrium transition to dipolar field lines in a future study.

[20] There are some timing studies that support the NENL model outside of what we have focused on. Also, many other observations such as the arrival of fast parallel flows prior to perpendicular flows [e.g., *Machida et al.*, 1999] are in agreement with our simulations. On the other hand, some observations [e.g., *Ohtani et al.*, 1999] open up new questions such as, what process is responsible for the explosive ground onset. Based on our results, we propose that a combination of the early parallel ion fluxes and parallel currents is a good candidate. It does not require a secondary CD mechanism.

[21] **Acknowledgments.** This work was supported by the NASA SEC Theory Program NAG5-11754, NASW-98018, and NSF grant ATM-9901665. Computational work was partially performed on San Diego Supercomputer Center resources, including the T3E and Blue Horizon. The authors thank Kevin Quest for useful discussions.

References

Akasofu, S.-I., The development of the auroral substorm, *Planet. Space Sci.*, 12,273–12,282, 1964.

Arzner, K., and M. Scholer, Kinetic structure of the post plasmoid plasma sheet during magnetotail reconnection, *J. Geophys. Res.*, *106*, 3827–3844, 2001.

Baker, D. N., T. I. Pulkkinen, V. Angelopoulos, W. Baumjohann, and R. L. McPherron, Neutral line model of substorms: Past results and present view, *J. Geophys. Res.*, *101*, 12,975–13,010, 1996.

Friedrich, E., J. C. Samson, I. Voronkov, and G. Rostoker, Dynamics of the substorm expansive phase, *J. Geophys. Res.*, *106*, 13,145–13,163, 2001.

Haerendel, G., Disruption, ballooning or auroral avalanche—On the cause of substorms, in *Substorms 1*, *Eur. Space Agency Spec. Publ.*, *ESA SP 335*, 417, 1992.

Hesse, M., and J. Birn, On dipolarization and its relation to the substorm current wedge, *J. Geophys. Res.*, *96*, 19,417–19,426, 1991.

Hones, E. W., Jr., The magnetotail: Its generation, and dissipation, in *Physics of Solar Planetary Environments*, vol. II, edited by D. J. Williams, pp. 558–571, AGU, Washington, D. C., 1976.

Hones, E. W., Jr., D. N. Baker, S. J. Bame, W. C. Feldman, J. T. Gosling, D. J. McComas, R. D. Zwickl, J. A. Slavin, E. J. Smith, and B. T. Tsurutani, Structure of the magnetotail at 220 R_E and its response to geomagnetic activity, *Geophys. Res. Lett.*, *11*, 5–7, 1984.

Krauss-Varban, D., H. Karimabadi, and N. Omidi, Two-dimensional structure of the co-planar and non-coplanar magnetopause transition during reconnection, *Geophys. Res. Lett.*, *26*, 1235–1238, 1999.

Lopez, R. E., H. Lühr, B. J. Anderson, P. T. Newell, and R. W. McEntire, Multipoint observations of small substorms, *J. Geophys. Res.*, *95*, 18,897–18,912, 1990.

Lopez, R. E., H. E. Spence, and C.-I. Meng, DMSP F7 observations of a substorm field-aligned current, *J. Geophys. Res.*, *96*, 19,409–19,415, 1991.

Lui, A. T. Y., Current disruption in the Earth's magnetosphere: Observations and models, *J. Geophys. Res.*, *101*, 13,067–13,088, 1996.

Machida, S., Y. Miyashita, A. Ieda, A. Nishida, T. Mukai, Y. Saito, and S. Kokubun, GEOTAIL observations of flow velocity and north-south magnetic field variations in the near and mid-distant tail associated with substorm onsets, *Geophys. Res. Lett.*, *26*, 635–638, 1999.

Miyashita, Y., S. Machida, A. Nishida, T. Mukai, Y. Saito, and S. Kokubun, Geotail observations of total pressure and electric field variations in the near and mid-distant tail associated with substorm onset, *Geophys. Res. Lett.*, *26*, 639–642, 1999.

Newell, P. T., K. Liou, T. Sotirelis, and C.-I. Meng, Auroral precipitation power during substorms: A Polar UV Imager-based superposed epoch analysis, *J. Geophys. Res.*, *106*, 28,885–28,896, 2001.

Ohtani, S., F. Creutzberg, T. Mukai, H. Singer, A. T. Y. Lui, M. Nakamura, P. Prikryl, K. Yumoto, and G. Rostoker, Substorm onset timing: The December 31, 1995, event, *J. Geophys. Res.*, *104*, 22,713–22,727, 1999.

Pulkkinen, T. I., D. N. Baker, L. L. Cogger, L. A. Fank, J. B. Sigwarth, S. Kokubun, T. Mukai, H. J. Singer, J. A. Slavin, and L. Zelenyi, Spatial extent and dynamics of a thin current sheet during the substorm growth phase on December 10, 1996, *J. Geophys. Res.*, *104*, 28,475–28,490, 1999.

Samson, J. C., L. R. Lyons, P. T. Newell, F. Creutzberg, and B. Xu, Proton aurora and substorm intensifications, *Geophys. Res. Lett.*, *19*, 2167–2170, 1992.

Shiokawa, K., et al., High-speed ion flow, substorm current wedge, and multiple Pi2 pulsations, *J. Geophys. Res.*, *103*, 4491–4507, 1998.

Ueno, G., S. Machida, T. Mukai, Y. Saito, and A. Nishida, Distribution of X-type magnetic neutral lines in the magnetotail with Geotail observations, *Geophys. Res. Lett.*, *26*, 3341–3344, 1999.

Wanliss, J. A., J. C. Samson, and E. Friedrich, On the use of photometer data to map dynamics of the magnetotail current sheet during substorm growth phase, *J. Geophys. Res.*, *105*, 27,673–27,784, 2000.

Zwingmann, W., J. Wallace, K. Schindler, and J. Birn, Particle simulation of magnetic reconnection in the magnetotail configuration, *J. Geophys. Res.*, *95*, 20,877–20,888, 1990.

H. Karimabadi and D. Krauss-Varban, Department of Electrical and Computer Engineering, University of California, San Diego, 9500 Gilman Dr., La Jolla, CA 92093-0407, USA. (varban@ece.ucsd.edu)